Adaptive Modulation and Joint Temporal Spatial Power Allocation for OSTBC MIMO Systems with Imperfect CSI

Quan Kuang, Shu-Hung Leung, and Xiangbin Yu

***Abstract*—We propose a novel adaptive transmission scheme for space-time coded multiple-input multiple-output beamforming systems with imperfect channel state information at the transmitter, of which the signal constellation, total transmit power (temporal power), and power allocation among eigen-beams (spatial power) are jointly adapted to maximize the average spectral efficiency, subject to a target bit-error-rate and an average power constraint. The power allocation over the spatial and temporal domains makes the traditional approach of partitioning the received signal-to-noise ratio (SNR) inapplicable to the above design problem. By introducing a new variable, called as effective signal-to-noise-to-modulation ratio (ESNMR), we derive a rate-selection policy by partitioning the range of the ESNMR with an optimal set of thresholds. A closed-form temporal power control policy and a simple spatial power allocation algorithm are also obtained. Numerical results demonstrate that the new adaptive transmission scheme yields a significant performance gain over existing adaptation systems.**

***Index Terms*—Adaptive modulation, orthogonal space-time block coding (OSTBC), multiple-input multiple-output (MIMO), beamforming, imperfect CSI, power allocation.**

I. Introduction

THE increasing demand of high data rate services always looks for spectrally efficient communication systems under limited radio spectrum. Adaptive modulation (AM), as a powerful technique for improving spectral efficiency (SE), has attracted lots of research efforts for single-input single-output (SISO) systems [1]–[5]. The channel state information (CSI) at the transmitter (CSIT) is crucial to the operation of AM, which may be obtained through a feedback channel. In practical systems, CSIT suffers from imperfection due to channel estimation errors, feedback delay, or quantization errors [6]. Imperfect CSI can adversely affect AM performance. Therefore, it should be taken into account explicitly in performing system design.

Paper approved by J. Wang, the Editor for Wireless Spread Spectrum of the IEEE Communications Society. Manuscript received January 18, 2011; revised December 14, 2011 and February 21, 2012.

The work of X. Yu was supported in part by the Doctoral Fund of the Ministry of Education of China under Grant 20093218120021, and in part by the National Natural Science Foundation of China under Grant 61172077.

Q. Kuang was with the City University of Hong Kong. He is now with the Institute of Telecommunications, University of Stuttgart, 70569 Stuttgart, Germany (e-mail: quan.kuang.box@gmail.com).

S. H. Leung is with the State Key Laboratory of Millimeter Wave and Department of Electronic Engineering, City University of Hong Kong (e-mail: eeeugshl@cityu.edu.hk).

X. Yu is with the Nanjing University of Aeronautics and Astronautics, Nanjing 210016, China (e-mail: yxbxwy@gmail.com).

Digital Object Identifier 10.1109/TCOMM.2012.050812.110044

Multiple-input multiple-output (MIMO) approach is another promising SE technique with diversity and coding benefits. Therefore, AM and MIMO can be combined to leverage both of their potentials. Among all the MIMO signaling schemes, orthogonal space-time block coding (OSTBC[1]) has been widely used due to its simplicity. Although OSTBC is a diversity-based scheme which aims at minimizing bit-error-rate (BER) at fixed spectral efficiency, it can be combined with AM to achieve high spectral efficiency for a target BER [7]–[11]. Actually, at low SNRs, OSTBC can yield higher spectral efficiency than spatial multiplexing scheme [11]. In [10], the performance of a variable-power (in time) variable-rate OSTBC system is analyzed under imperfect CSI. However, none of the above systems consider the power allocation among transmit antennas. Without the spatial power allocation, these works can use received signal-to-noise ratio (SNR) to derive adaptation policies by partitioning the range of SNR, parallel to the previous SISO cases. It is well-known that the BER performance of OSTBC systems can be improved by spatial power allocation for fixed data rate transmission [12]. Intuitively speaking, if we combine spatio-temporal power allocation with AM for OSTBC systems, the SE can be further increased for given target BER and average power constraint. However, this design problem is difficult and has not yet been solved.

Making use of CSIT, the OSTBC has been combined with beamforming (BF) to provide robustness against imperfection in CSIT [6], [13], [14]. The outputs of the OSTBC, after being power loaded, are transmitted through the eigen-directions of the autocorrelation matrix of the spatial channel estimate. AM for OSTBC-BF systems has been investigated in [15]. In order to alleviate the difficulty incurred by spatio-temporal power allocation, [15] focuses on constant-power transmission, only adjusting the constellation size and spatial power allocation. Though the time domain freedom is put aside, the constant-power AM-MIMO problem has been solved by trial and error: start with the largest constellation and calculate the expected BER with optimal spatial power allocation, then decrease the constellation size until the target BER is satisfied. However, this constant-power approach restricts the system performance. In other words, the existing AM schemes for OSTBC or OSTBC-BF systems lack of an efficient design algorithm and do not fully utilize the degrees of freedom of spatial

[1]OSTBC denotes orthogonal space-time block coding/coded/code/codes according to the context.

and temporal power adaptation, which results in performance inferiority.

In this paper, we develop optimal AM schemes for OSTBC/OSTBC-BF MIMO systems with joint spatio-temporal power allocation under imperfect CSI. The constellation size, total transmit power and spatial power allocation parameters are jointly optimized to maximize the average spectral efficiency (ASE), subject to a target BER and an average power constraint. The initial formulation seems to be complicated. However, by introducing a new variable, called as effective signal-to-noise-to-modulation ratio (ESNMR), we can modify the original problem as an inner-outer optimization problem resulting in an efficient solution. Employing this variable, we can derive a rate-selection policy by partitioning the range of the ESNMR with optimal thresholds. A closed-form temporal power control policy and a simple spatial power allocation algorithm are also obtained. The complexity of the proposed variable-rate and variable-power adaptation algorithm is reduced to one-dimensional root-finding of a monotonic function.

The rest of this paper is organized as follows. In Section II, the system model is introduced and the problem is formulated. The variable-rate spatio-temporal power adaptation algorithm is developed in Section III. Numerical results and practical issue of peak power constraint are discussed in Section IV. Finally, we conclude the paper in Section V.

Notation: Bold upper case and lower case letters denote matrices and vectors, respectively. The superscript $(\cdot)^H$ denotes the Hermitian transposition. $\|\cdot\|_F$ denotes the Frobenius norm of a matrix. $E[\cdot]$ denotes the expectation. $\mathrm{tr}(\cdot)$ denotes the trace of a matrix. $\mathbf{I}_N$ is the $N \times N$ identity matrix.

II. System Description

A. System Model

We consider a wireless multi-antenna communication system with N_t transmit antennas and N_r receive antennas operating over a flat and quasi-static Rayleigh fading channel as depicted in Fig.1. The adaptive modulator in the system employs M-ary quadrature amplitude modulation (MQAM). The space-time encoder, which is represented by an $N_\mathrm{t} \times T$ OSTBC transmission codeword matrix [16], is used to encode K data symbols into an N_t-dimensional vector sequence of T time slots with code rate $r = K/T$. The OSTBC vector sequence is then sent along the N_t eigen-directions of the autocorrelation matrix of the spatial channel estimate at the transmitter with power allocation in space and time.

The channel is represented by an $N_\mathrm{r} \times N_\mathrm{t}$ matrix $\mathbf{H} = \{h_{ij}\}$, where h_{ij} denotes the channel gain from the jth transmit antenna to the ith receive antenna. It is assumed that h_{ij} remains constant over an OSTBC frame and varies from frame to frame, and $\{h_{ij}\}$ are modeled as independent identically distributed (i.i.d.) complex Gaussian random variables (r.v.s) with zero-mean and variance 0.5 per dimension. At the transmitter, only an imperfect channel estimate $\hat{\mathbf{H}}$ is available for the current frame, modeled as $\hat{\mathbf{H}} = \mathbf{H}+\mathbf{E}$ [9], [17], where $\mathbf{E}$ is the channel error matrix independent of $\mathbf{H}$. The elements of $\mathbf{E}$ are assumed to be i.i.d. complex Gaussian r.v.s with zero mean and variance σ_e^2.

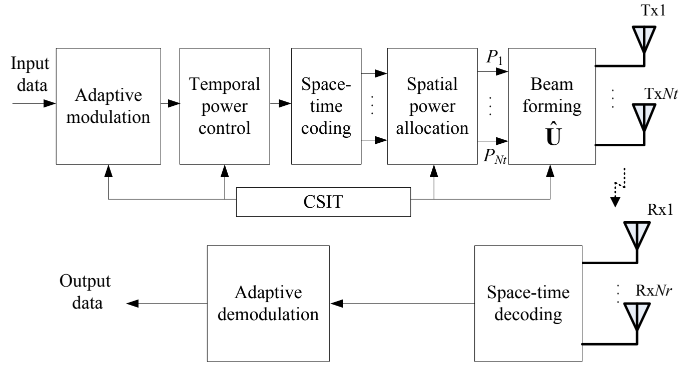

Fig. 1. System diagram.

Let $\mathbf{h} = \mathrm{vec}(\mathbf{H})$, $\hat{\mathbf{h}} = \mathrm{vec}(\hat{\mathbf{H}})$, and $\mathbf{e} = \mathrm{vec}(\mathbf{E})$ be the column vectors constructed by stacking the columns of $\mathbf{H}$, $\hat{\mathbf{H}}$, and $\mathbf{E}$ respectively. Based on the Bayesian Linear Model and Theorem 10.3 in [18], the mean and covariance matrices of $\mathbf{h}$ given $\hat{\mathbf{h}}$ are given as

$$E[\mathbf{h}|\hat{\mathbf{h}}] = \mathbf{C_h}(\mathbf{C_h}+\mathbf{C_e})^{-1}\hat{\mathbf{h}} = (1+\sigma_e^2)^{-1}\hat{\mathbf{h}} \quad (1)$$

$$\mathbf{C}_{\mathbf{h}|\hat{\mathbf{h}}} = \mathbf{C_h} - \mathbf{C_h}(\mathbf{C_h}+\mathbf{C_e})^{-1}\mathbf{C_h} = \sigma_e^2(1+\sigma_e^2)^{-1}\mathbf{I}_{N_\mathrm{r}N_\mathrm{t}} \quad (2)$$

where $\mathbf{C_e} = \sigma_e^2\mathbf{I}_{N_\mathrm{r}N_\mathrm{t}}$ and $\mathbf{C_h} = \mathbf{I}_{N_\mathrm{r}N_\mathrm{t}}$ are the covariance matrices of $\mathbf{e}$ and $\mathbf{h}$ respectively. Hence, conditioned on $\hat{\mathbf{H}}$, the elements $\{h_{ij}\}$ of $\mathbf{H}$ are complex Gaussian r.v.s with mean $(1+\sigma_e^2)^{-1}\hat{h}_{ij}$ and variance $\sigma_e^2(1+\sigma_e^2)^{-1}$.

The received signals of the system can be expressed as

$$\mathbf{Y} = \sqrt{S}\mathbf{H}\hat{\mathbf{U}}\mathbf{P}\mathbf{D} + \mathbf{Z} = \sqrt{S}\bar{\mathbf{H}}\mathbf{P}\mathbf{D} + \mathbf{Z} \quad (3)$$

where $\bar{\mathbf{H}} \triangleq \mathbf{H}\hat{\mathbf{U}}$, $\hat{\mathbf{U}} = \{\hat{u}_{ij}\}$ is an $N_\mathrm{t} \times N_\mathrm{t}$ unitary matrix containing the N_t-eigenvectors of $\hat{\mathbf{H}}^H\hat{\mathbf{H}}$ corresponding to the eigenvalues $\{\hat{\zeta}_j\}$ sorted in decreasing order, $\mathbf{D}$ is the OSTBC codeword matrix with normalized average power as $E[\mathrm{tr}(\mathbf{D}\mathbf{D}^H)]/T = 1$, $\mathbf{Z}$ is an $N_\mathrm{r} \times T$ received noise matrix with i.i.d. entries modeled as complex Gaussian r.v.s with zero mean and variance σ_n^2, S is the total transmit power radiated from the N_t transmit antennas, $\mathbf{Y}$ is the $N_\mathrm{r} \times T$ received signal matrix, and $\mathbf{P} = \mathrm{diag}(\sqrt{P_1}, \sqrt{P_2}, \ldots, \sqrt{P_{N_\mathrm{t}}})$ denotes a diagonal power allocation matrix which satisfies

$$\sum_{j=1}^{N_\mathrm{t}} P_j = 1, \quad P_j \geq 0, \quad \forall j. \quad (4)$$

It is assumed that the receiver perfectly knows the CSI. After space-time decoding, the instantaneous received SNR per symbol at the receiver is expressed as [19]

$$\rho = \frac{S}{r\sigma_n^2}\|\bar{\mathbf{H}}\mathbf{P}\|_F^2 = \frac{S}{r\sigma_n^2}\sum_{j=1}^{N_\mathrm{t}} P_j\beta_j \quad (5)$$

where β_j is the jth eigen-channel power gain defined as

$$\beta_j = \sum_{i=1}^{N_\mathrm{r}} |\bar{h}_{ij}|^2 = \sum_{i=1}^{N_\mathrm{r}} |\sum_{\nu=1}^{N_\mathrm{t}} h_{i\nu}\hat{u}_{\nu j}|^2. \quad (6)$$

If we consider OSTBC without beamforming, (6) becomes $\beta_j = \sum_{i=1}^{N_\mathrm{r}} |h_{ij}|^2$, which is the channel power gain of the jth transmit antenna.

Now we derive the conditional probability density function (pdf) of β_j in (6) given $\hat{\mathbf{H}}$. According to (1), (2) and $\bar{\mathbf{H}} \triangleq \mathbf{H}\hat{\mathbf{U}}$, the mean and covariance matrix of $\bar{\mathbf{h}} = \text{vec}(\bar{\mathbf{H}})$ conditioned on $\hat{\mathbf{h}}$ can be written as

$$\mathbf{m}_{\bar{\mathbf{h}}|\hat{\mathbf{h}}} = E[\text{vec}(\mathbf{H}\hat{\mathbf{U}})|\hat{\mathbf{h}}] = (1+\sigma_e^2)^{-1}\text{vec}(\hat{\mathbf{H}}\hat{\mathbf{U}}) \quad (7)$$

$$\mathrm{C}_{\bar{\mathbf{h}}|\hat{\mathbf{h}}} = \sigma_e^2(1+\sigma_e^2)^{-1}\mathbf{I}_{N_\mathrm{r}N_\mathrm{t}}. \quad (8)$$

Hence, conditioned on $\hat{\mathbf{H}}$, the elements $\{\bar{h}_{ij}\}$ of $\bar{\mathbf{H}}$ become i.i.d. complex Gaussian r.v.s with mean $(1+\sigma_e^2)^{-1}\sum_{\nu=1}^{N_\mathrm{t}} \hat{h}_{i\nu}\hat{u}_{\nu j}$ and variance $\sigma_e^2(1+\sigma_e^2)^{-1}$. Thus given $\hat{\mathbf{H}}$, $\{\beta_j\}$ in (6) are independent noncentral chi-square r.v.s. Utilizing Eq.(2.1-118) in [20], the conditional pdf of β_j given $\hat{\mathbf{H}}$ is

$$f_{\beta_j|\hat{\mathbf{H}}}(\beta_j|\hat{\mathbf{H}}) = \frac{1}{\sigma^2}\left(\frac{\beta_j}{\tilde{\beta}_j}\right)^{\frac{N_\mathrm{r}-1}{2}} e^{-\frac{\tilde{\beta}_j+\beta_j}{\sigma^2}} I_{N_\mathrm{r}-1}\left(\frac{2\sqrt{\tilde{\beta}_j\beta_j}}{\sigma^2}\right), \quad j=1,\ldots,\min\{N_\mathrm{r},N_\mathrm{t}\} \quad (9)$$

where the variance σ^2 and the sum of squared means, denoted by $\tilde{\beta}_j$, are given by

$$\sigma^2 = \sigma_e^2(1+\sigma_e^2)^{-1} \quad (10)$$

$$\tilde{\beta}_j = \sum_{i=1}^{N_\mathrm{r}} |\sum_{\nu=1}^{N_\mathrm{t}} \hat{h}_{i\nu}\hat{u}_{\nu j}|^2(1+\sigma_e^2)^{-2} = \hat{\zeta}_j(1+\sigma_e^2)^{-2}, \quad (11)$$

$\tilde{\beta}_1 \geq \tilde{\beta}_2 \cdots \geq \tilde{\beta}_{N_\mathrm{t}}$ since $\hat{\zeta}_1 \geq \hat{\zeta}_2 \cdots \geq \hat{\zeta}_{N_\mathrm{t}}$, and $I_v(x)$ is the vth order modified Bessel function of the first kind [20]. For systems with $N_\mathrm{t} > N_\mathrm{r}$, there are $N_\mathrm{t}-N_\mathrm{r}$ beams with $\hat{\zeta}_j = 0$. Given $\hat{\mathbf{H}}$, $\{\beta_j\}$ of those beams are independent central chi-square distributed, with the conditional pdf given as [20]

$$f_{\beta_j|\hat{\mathbf{H}}}(\beta_j|\hat{\mathbf{H}}) = \frac{\beta_j^{N_\mathrm{r}-1}}{\sigma^{2N_\mathrm{r}}\Gamma(N_\mathrm{r})}e^{-\frac{\beta_j}{\sigma^2}}, \quad j=N_\mathrm{r}+1,\ldots,N_\mathrm{t}. \quad (12)$$

B. Problem Formulation

The BER for square MQAM of constellation size M with Gray mapping and received SNR ρ can be approximated by the tight upper bound [1], [7], [10], [15]: $\text{BER}_{\text{MQAM}} \approx 0.2\exp\left(-\frac{1.5\rho}{M-1}\right)$. With (5), the above approximation can be written as

$$\text{BER}_{\text{MQAM}} \approx 0.2\exp\left(-\gamma\sum_{j=1}^{N_\mathrm{t}} P_j\beta_j\right) \quad (13)$$

where an effective signal-to-noise-to-modulation ratio (ESNMR) is defined as

$$\gamma = \frac{1.5S}{(M-1)r\sigma_n^2}. \quad (14)$$

In this paper, our goal is to design variable-power and variable-rate control policies for the transmitter to adapt signal constellation size $M = M(\tilde{\boldsymbol{\beta}})$, transmit power $S = S(\tilde{\boldsymbol{\beta}})$ and spatial power allocation parameters $P_j = P_j(\tilde{\boldsymbol{\beta}})$ to maximize the average transmission rate according to the imperfect CSIT $\tilde{\boldsymbol{\beta}} = (\tilde{\beta}_1,\ldots,\tilde{\beta}_{N_\mathrm{t}})$, subject to average power and target BER constraints. The average BER given $\hat{\mathbf{H}}$ is expressed as

$$\text{BER} = \int \text{BER}_{\text{MQAM}}(M(\tilde{\boldsymbol{\beta}}),S(\tilde{\boldsymbol{\beta}}),P_j(\tilde{\boldsymbol{\beta}}),\boldsymbol{\beta})f_{\boldsymbol{\beta}|\hat{\mathbf{H}}}(\boldsymbol{\beta}|\hat{\mathbf{H}})d\boldsymbol{\beta} \quad (15)$$

where $f_{\boldsymbol{\beta}|\hat{\mathbf{H}}}(\boldsymbol{\beta}|\hat{\mathbf{H}})$ is the joint conditional pdf of $\{\beta_j\}$, given the channel estimate $\hat{\mathbf{H}}$. Applying (9), (12) and the independence of $\{\beta_j\}$ to (15), the average BER given $\hat{\mathbf{H}}$ can be expressed as (16), which will be used as a performance metric in the following,

$$\text{BER} = 0.2\prod_{j=1}^{N_\mathrm{t}}\frac{\exp\left(-\frac{\tilde{\beta}_j\gamma(\tilde{\boldsymbol{\beta}})P_j(\tilde{\boldsymbol{\beta}})}{1+\sigma^2\gamma(\tilde{\boldsymbol{\beta}})P_j(\tilde{\boldsymbol{\beta}})}\right)}{(1+\sigma^2\gamma(\tilde{\boldsymbol{\beta}})P_j(\tilde{\boldsymbol{\beta}}))^{N_\mathrm{r}}} \quad (16)$$

where $\gamma(\tilde{\boldsymbol{\beta}}) = \frac{1.5S(\tilde{\boldsymbol{\beta}})}{(M(\tilde{\boldsymbol{\beta}})-1)r\sigma_n^2}$.

For discrete-rate MQAM, we consider $L+1$ different QAM constellations with $M_l = 2^{k_l}$, $l=1,\ldots,L+1$, where $k_l \in \{0,2,4,\ldots,2L\}$, of which 2^0 corresponds to no transmission. We can partition the N_t-dimensional space of $\tilde{\boldsymbol{\beta}}$ into $L+1$ regions, $\{D_l, l=1,...,L+1\}$, each associated with one constellation. Specifically, we choose

$$M(\tilde{\boldsymbol{\beta}}) = M_l, \quad \text{for} \quad \tilde{\boldsymbol{\beta}} \in D_l. \quad (17)$$

Thus, the constrained ASE maximization problem is formulated as

$$\begin{aligned}
\underset{\{D_l\},S(\tilde{\boldsymbol{\beta}}),\{P_j(\tilde{\boldsymbol{\beta}})\}}{\text{maximize}} \quad & \sum_{l=1}^{L+1} r\log_2(M_l)\int_{D_l} f_{\tilde{\boldsymbol{\beta}}}(\tilde{\boldsymbol{\beta}})d\tilde{\boldsymbol{\beta}} \\
\text{subject to} \quad & \int S(\tilde{\boldsymbol{\beta}})f_{\tilde{\boldsymbol{\beta}}}(\tilde{\boldsymbol{\beta}})d\tilde{\boldsymbol{\beta}} = \bar{S},\ S(\tilde{\boldsymbol{\beta}}) \geq 0 \\
& \text{BER}_l \leq \text{BER}_{\text{tgt}}, \quad l=1,\ldots,L+1 \\
& \sum_{j=1}^{N_\mathrm{t}} P_j(\tilde{\boldsymbol{\beta}}) = 1, \quad P_j(\tilde{\boldsymbol{\beta}}) \geq 0\ \forall j \\
& M_l \in \{2^0,2^2,\ldots,2^{2L}\}
\end{aligned} \quad (18)$$

where $\bar{S}$ is the average transmit power, BER_l is obtained by inserting $\gamma(\tilde{\boldsymbol{\beta}}) = \frac{1.5S(\tilde{\boldsymbol{\beta}})}{(M_l-1)r\sigma_n^2}$ into (16), BER_{tgt} is the target BER, $f_{\tilde{\boldsymbol{\beta}}}(\tilde{\boldsymbol{\beta}})$ is the joint pdf of $\tilde{\boldsymbol{\beta}}$, which can be obtained from the joint pdf of ordered eigenvalues of the Wishart matrix, as shown in (54) in Appendix B.

Generally, it is not easy to specify the multi-dimensional boundaries of $\{D_l\}$ and the computation of the probability that $\tilde{\boldsymbol{\beta}}$ lies in $\{D_l\}$ is mathematically intractable because it involves multiple integrals over regions of arbitrary shapes. To solve this problem in next section, we will make use of the ESNMR parameter γ, defined in (14), to express the BER and constellation size. By doing so, the constrained maximization problem can be transformed to an inner-outer optimization problem with constraints being decoupled. This approach can help reduce the multi-dimensional partition problem to an one-dimensional partition problem.

III. Joint Rate and Spatio-Temporal Power Adaptation

In this section, we first study the continuous-rate case to obtain useful intuition for the discrete-rate case.

A. Continuous Rate

If we assume M can take any positive value satisfying $M \geq 2^0$, then the average transmission rate maximization problem for the continuous case is formulated as

$$\begin{aligned} \underset{M(\tilde{\boldsymbol{\beta}}),S(\tilde{\boldsymbol{\beta}}),\{P_j(\tilde{\boldsymbol{\beta}})\}}{\text{maximize}} \quad & \int r\log_2(M(\tilde{\boldsymbol{\beta}}))f_{\tilde{\boldsymbol{\beta}}}(\tilde{\boldsymbol{\beta}})d\tilde{\boldsymbol{\beta}} \\ \text{subject to} \quad & \int S(\tilde{\boldsymbol{\beta}})f_{\tilde{\boldsymbol{\beta}}}(\tilde{\boldsymbol{\beta}})d\tilde{\boldsymbol{\beta}} = \bar{S},\ S(\tilde{\boldsymbol{\beta}}) \geq 0 \\ & \text{BER}(M(\tilde{\boldsymbol{\beta}}),S(\tilde{\boldsymbol{\beta}}),P_j(\tilde{\boldsymbol{\beta}})) \leq \text{BER}_{\text{tgt}} \\ & \sum_{j=1}^{N_{\text{t}}} P_j(\tilde{\boldsymbol{\beta}}) = 1, \quad P_j(\tilde{\boldsymbol{\beta}}) \geq 0\ \forall j \\ & M(\tilde{\boldsymbol{\beta}}) \geq 2^0. \end{aligned} \tag{19}$$

The above constrained optimization problem is difficult to solve because the BER formula of (16) is complicated and the spatial and temporal power are coupled in the BER constraint. We now express M in terms of the transmission power S and parameter γ by using (14). Hence, the objective function in (19) can be expressed as

$$g(S(\tilde{\boldsymbol{\beta}}),\gamma(\tilde{\boldsymbol{\beta}})) = \int r\log_2\left(1+\frac{1.5S(\tilde{\boldsymbol{\beta}})}{r\sigma_n^2\gamma(\tilde{\boldsymbol{\beta}})}\right)f_{\tilde{\boldsymbol{\beta}}}(\tilde{\boldsymbol{\beta}})d\tilde{\boldsymbol{\beta}} \tag{20}$$

and the problem (19) now becomes

$$\underset{S(\tilde{\boldsymbol{\beta}}),\gamma(\tilde{\boldsymbol{\beta}}),\{P_j(\tilde{\boldsymbol{\beta}})\}}{\text{maximize}} \quad g(S(\tilde{\boldsymbol{\beta}}),\gamma(\tilde{\boldsymbol{\beta}})) \tag{21a}$$

$$\text{subject to} \quad \int S(\tilde{\boldsymbol{\beta}})f_{\tilde{\boldsymbol{\beta}}}(\tilde{\boldsymbol{\beta}})d\tilde{\boldsymbol{\beta}} = \bar{S},\ S(\tilde{\boldsymbol{\beta}}) \geq 0 \tag{21b}$$

$$\text{BER}(P_j(\tilde{\boldsymbol{\beta}}),\gamma(\tilde{\boldsymbol{\beta}})) \leq \text{BER}_{\text{tgt}} \tag{21c}$$

$$\sum_{j=1}^{N_{\text{t}}} P_j(\tilde{\boldsymbol{\beta}}) = 1, \quad P_j(\tilde{\boldsymbol{\beta}}) \geq 0\ \forall j \tag{21d}$$

$$\gamma(\tilde{\boldsymbol{\beta}}) \geq 0. \tag{21e}$$

Note that the constraints in (21b) depend only on $S(\tilde{\boldsymbol{\beta}})$, while the constraints in (21c)-(21e) depend on $\gamma(\tilde{\boldsymbol{\beta}})$ and $P_j(\tilde{\boldsymbol{\beta}})$. The spatial power and temporal power are now decoupled in the constraints. Hence, the maximization problem of (21) can be expressed as an inner-outer problem as follows

$$\begin{aligned} \underset{S(\tilde{\boldsymbol{\beta}})\geq 0}{\text{maximize}} \quad & \tilde{g}(S(\tilde{\boldsymbol{\beta}})) \\ \text{subject to} \quad & \int S(\tilde{\boldsymbol{\beta}})f_{\tilde{\boldsymbol{\beta}}}(\tilde{\boldsymbol{\beta}})d\tilde{\boldsymbol{\beta}} = \bar{S} \end{aligned} \tag{22}$$

where

$$\tilde{g}(S) = \sup_{\gamma,\{P_j\}} \{g(S,\gamma)|\text{BER}(P_j,\gamma) \leq \text{BER}_{\text{tgt}}, \gamma \geq 0, \sum_{j=1}^{N_{\text{t}}} P_j = 1, P_j \geq 0\} \tag{23}$$

and we drop the dependence of $\tilde{\boldsymbol{\beta}}$ in (23) and the sequel for simplicity unless there is ambiguity.

Note that for fixed S, maximizing $g(S,\gamma)$ subject to the constraints from (21c) to (21e) is equivalent to maximizing $\log_2\left(1+\frac{1.5S}{r\sigma_n^2\gamma}\right)$ for any given $\tilde{\boldsymbol{\beta}}$, because these constraints are imposed on every realization of $\tilde{\boldsymbol{\beta}}$. Furthermore, $\log_2\left(1+\frac{1.5S}{r\sigma_n^2\gamma}\right)$ is a monotonically decreasing function of γ for fixed S. Hence, (23) can be obtained by solving the following inner minimization problem for every realization of $\tilde{\boldsymbol{\beta}}$:

$$\begin{aligned} \underset{\gamma\geq 0,\{P_j\geq 0\}}{\text{minimize}} \quad & \gamma \\ \text{subject to} \quad & \text{BER}(P_j,\gamma) \leq \text{BER}_{\text{tgt}}, \quad \sum_{j=1}^{N_{\text{t}}} P_j = 1. \end{aligned} \tag{24}$$

We show in Appendix A that the solution to the optimization problem of (24) is

$$\gamma^\star = \frac{1}{\sigma^2}\left(\sum_{j=1}^{\bar{N}_{\text{t}}} \mathcal{I}_j(\lambda^\star) - \bar{N}_{\text{t}}\right) \tag{25}$$

$$P_j^\star = \max\left\{0, \frac{1}{\sigma^2\gamma^\star}\left(\mathcal{I}_j(\lambda^\star)-1\right)\right\} \tag{26}$$

where

$$\mathcal{I}_j(\lambda) = \frac{\sqrt{N_{\text{r}}^2\sigma^4 + 4\tilde{\beta}_j\lambda} + N_{\text{r}}\sigma^2}{2\lambda} \tag{27}$$

and $\lambda^\star$ is the positive root of the following monotonically increasing function:

$$F_{\bar{N}_{\text{t}}}(\lambda) = \log\frac{0.2}{\text{BER}_{\text{tgt}}} - \sum_{j=1}^{\bar{N}_{\text{t}}}\left(N_{\text{r}}\log\mathcal{I}_j(\lambda) - \frac{\tilde{\beta}_j}{\mathcal{I}_j(\lambda)\sigma^2} + \frac{\tilde{\beta}_j}{\sigma^2}\right). \tag{28}$$

Notice that the positive root always exists and is unique since $F_{\bar{N}_{\text{t}}}(0^+) = -\infty$ and $F_{\bar{N}_{\text{t}}}(\infty) = \infty$. If $\{P_j^\star\}_{j=1,\ldots,\bar{N}_{\text{t}}}$ are positive, then $\gamma^\star$ is positive. $\bar{N}_{\text{t}}$ is the number of eigen-beams allocated with nonzero power. To determine the value of $\bar{N}_{\text{t}}$, we can use the following conventional iterative Algorithm 1.

Algorithm 1 of finding $\gamma^\star$ and $\{P_j^\star\}$ for given $\tilde{\boldsymbol{\beta}}$

(i) Initially set $\bar{N}_{\text{t}} = N_{\text{t}}$.

(ii) Obtain the root of the monotonic function $F_{\bar{N}_{\text{t}}}(\lambda)$ numerically by Newton's method (or bisection method), denoted as λ°. Substituting λ° into (25) and (26) obtains γ and $\{P_j\}$. If $\{P_j\}$ all are positive, then $\lambda^\star = \lambda^\circ$ and $\gamma^\star = \gamma$, $P_j^\star = P_j$; otherwise go to step (iii).

(iii) Set $\bar{N}_{\text{t}} = \bar{N}_{\text{t}} - 1$ and go to step (ii).

The above procedure needs to compute the root for each iteration during the determination of $\bar{N}_{\text{t}}$. To reduce the computational complexity, we provide the following theorem which gives a necessary and sufficient condition to determine the value of $\bar{N}_{\text{t}}$ without resort to iterative calculation.

Theorem 1: The optimal $\{P_j^\star,\ j=1,\ldots,\bar{N}_{\text{t}}\}$ are positive if and only if $F_{\bar{N}_{\text{t}}}(\lambda_{\bar{N}_{\text{t}}}^{(u)}) > 0$, where $\bar{N}_{\text{t}} = \arg\max_\nu F_\nu(\lambda_\nu^{(u)}) > 0$, $F_\nu(\lambda)$ is given by (28), and $\lambda_\nu^{(u)}$ is an upper bound of $\lambda^\star$ defined as $\lambda^\star < N_{\text{r}}\sigma^2 + \tilde{\beta}_\nu \triangleq \lambda_\nu^{(u)},\ \nu = 1,\ldots,N_{\text{t}}$.

Proof: The proof is based on the monotonically increasing property of $F_{\bar{N}_{\text{t}}}(\lambda)$, and omitted here due to lack of space. ■

Thanks to Theorem 1, the algorithm that solves the inner optimization problem can determine the value of $\bar{N}_{\text{t}}$ directly and calculate only once the root of $F_{\bar{N}_{\text{t}}}(\lambda)$ numerically to obtain $\lambda^\star$. The whole algorithm of obtaining $\gamma^\star$ and $\{P_j^\star\}$ is now summarized as follows.

Algorithm 2 of finding $\gamma^\star$ and $\{P_j^\star\}$ for given $\tilde{\boldsymbol{\beta}}$

(i) Starting from $\nu = N_\mathrm{t}$ to $\nu = 1$, determine the largest ν such that $F_\nu(\lambda_\nu^{(u)}) > 0$ and let $\bar{N}_\mathrm{t} = \nu$.
(ii) Use Newton's method (or bisection method) to solve $F_{\bar{N}_\mathrm{t}}(\lambda) = 0$ to obtain $\lambda^\star$.
(iii) Compute $\gamma^\star$ using (25).
(iv) Compute $\{P_j^\star\}$ using (26).

The outer optimization problem of (22) can be solved by the Calculus of Variations [22]. We define $J(S(\tilde{\boldsymbol{\beta}})) = \left[r\log_2\left(1+\frac{1.5S(\tilde{\boldsymbol{\beta}})}{r\sigma_n^2\gamma^\star(\tilde{\boldsymbol{\beta}})}\right)+\xi(\bar{S}-S(\tilde{\boldsymbol{\beta}}))\right]f_{\tilde{\boldsymbol{\beta}}}(\tilde{\boldsymbol{\beta}})$, where ξ is a Lagrange multiplier. Note that J is concave in $S(\tilde{\boldsymbol{\beta}})$. By setting $\partial J/\partial S(\tilde{\boldsymbol{\beta}}) = 0$, we obtain the global maximizer as

$$S^\star(\tilde{\boldsymbol{\beta}}) = \left(\frac{r}{\xi\log 2} - \frac{r\sigma_n^2\gamma^\star(\tilde{\boldsymbol{\beta}})}{1.5}\right)^+ = \frac{r\sigma_n^2}{1.5}(\gamma_0 - \gamma^\star(\tilde{\boldsymbol{\beta}}))^+ \tag{29}$$

where $(x)^+ = \max(x, 0)$ and γ_0 is a constant. According to (14), the optimal rate adaptation policy is

$$M^\star(\tilde{\boldsymbol{\beta}}) = \max\left(\frac{\gamma_0}{\gamma^\star(\tilde{\boldsymbol{\beta}})}, 1\right). \tag{30}$$

From (29) and (30), we can see that whenever $\gamma^\star(\tilde{\boldsymbol{\beta}})$ is beyond γ_0, no transmission occurs. Thus, γ_0 is referred to as threshold, whose value can be found by substituting (29) into the average power constraint in (22) and solving the resulting equation

$$\int \frac{r\sigma_n^2}{1.5}(\gamma_0 - \gamma^\star(\tilde{\boldsymbol{\beta}}))^+ f_{\tilde{\boldsymbol{\beta}}}(\tilde{\boldsymbol{\beta}})d\tilde{\boldsymbol{\beta}} = \bar{S}. \tag{31}$$

Since the left-hand side of (31) is a monotonically increasing function of γ_0, a unique solution of γ_0 exits and can be found numerically. The integration can be calculated by Gauss-Laguerre method [23] or the Monte-Carlo method. We provide in Appendix B the mathematical details of the numerical calculation.

Remark 1: From (29) and (30) we observe that the obtained adaptation policies actually use larger constellation size and higher transmit power when $\gamma^\star$ is small, and vice versa. This adaptation strategy can be explained intuitively as follows. From the definition of γ expressed as (14), assuming the current channel state needs a large $\gamma^\star$ to satisfy the BER requirement, the system will consume a large amount of transmit power S if the constellation size is not reduced, causing inefficient power consumption. Therefore, the optimal adaptation policy prefers to reduce the constellation size in order to save transmit power. Even more, it may decide not to use the current channel state for transmission if it requires too large power (when $\gamma^\star > \gamma_0$). Hence, $\gamma^\star$ can be regarded as a channel quality indicator for given BER requirement.

B. Discrete Rate

By introducing the same new variable γ in (14) to the discrete rate problem of (18), we can separate it into an inner optimization problem which is the same as (24) and an outer one. As mentioned previously, $\gamma^\star$ can be regarded as an indicator to reflect the channel fading quality. This motivates us to solve the outer optimization problem based on the value of $\gamma^\star$. Specifically, we partition the range of $\gamma^\star$ values into $L+1$ regions with boundaries $\{\gamma_0 = 0, \gamma_1, \ldots, \gamma_L, \gamma_{L+1} = \infty\}$, and assign constellation M_l to the lth region $[\gamma_{l-1}, \gamma_l)$ $(1 \le l \le L+1)$, giving the data rate $rk_l = r\log_2(M_l)$ bits/symbol. As discussed in Section III-A, the smaller the $\gamma^\star$, the larger the constellation size M should be. So we have $M_1 > M_2 \cdots > M_{L+1}$. The discrete-rate outer optimization problem is now reformulated as

$$\underset{\{\gamma_l\}}{\text{maximize}} \quad \sum_{l=1}^{L+1} r\log_2(M_l)\int_{\gamma_{l-1}}^{\gamma_l} p(\gamma^\star)d\gamma^\star \tag{32a}$$

$$\text{subject to} \quad \sum_{l=1}^{L+1}\int_{\gamma_{l-1}}^{\gamma_l} S(\gamma^\star)p(\gamma^\star)d\gamma^\star = \bar{S} \tag{32b}$$

$$S(\gamma^\star) = \frac{(M_l-1)r\sigma_n^2\gamma^\star}{1.5}, \gamma_{l-1} \le \gamma^\star < \gamma_l \tag{32c}$$

$$M_1 > M_2 \cdots > M_{L+1}. \tag{32d}$$

where $p(\gamma^\star)$ is the pdf of $\gamma^\star$.

The optimal thresholds $\{\gamma_l\}_{l=1}^L$ can be obtained by using the Lagrangian method [2, Section VI-D] [10], resulting in

$$\gamma_l = \mu\frac{1.5(k_l - k_{l+1})}{\sigma_n^2(M_l - M_{l+1})} = \mu t_l \tag{33}$$

where

$$t_l \triangleq \frac{1.5(k_l - k_{l+1})}{\sigma_n^2(M_l - M_{l+1})}, \quad l = 1, \ldots, L$$

and we define $t_0 = 0, t_{L+1} = \infty$. The μ parameter is the positive Lagrangian multiplier determined by substituting (33) and (32c) into the average power constraint (32b) and solving the resulting equation. We denote the left-hand side of the equation as $\psi(\mu)$. It is easily proved that $\psi(\mu)$ is a monotonically increasing function of μ, with $\psi(0) = 0$ and $\psi(\infty) = \frac{(M_1-1)r\sigma_n^2}{1.5}\int_0^\infty \gamma^\star p(\gamma^\star)d\gamma^\star$. Thus, the existence condition of the Lagrangian multiplier is $\psi(\infty) > \bar{S}$. If it is satisfied, the solution of μ is unique. Although closed-form of $p(\gamma^\star)$ is not available, we can calculate the integration numerically. Appendix C provides the details of finding μ. Once μ is obtained, it can be inserted into (33) to get the optimal boundaries. On the other hand, if $\psi(\infty) < \bar{S}$, it means that we can choose the largest modulation M_1 for all the channel realizations, while still keeping the average power below the power budget. This happens when σ_n^2 is very small (high SNR regions). Under this circumstance, the optimal boundaries become $\{\gamma_0 = 0, \gamma_1 = \infty\}$.

After we obtain the optimal boundaries, the discrete rate adaptive transmission design is completed. Now we summarize the adaptation policy for the discrete-rate case as follows.

(i) Use the algorithm 2 proposed in Section III-A to find $\gamma^\star$ and $\{P_j^\star\}$ for given CSIT $\tilde{\boldsymbol{\beta}}$.
(ii) Choose M_l when $\gamma^\star \in [\gamma_{l-1}, \gamma_l)$.
(iii) Compute $S(\gamma^\star)$ using (32c).

C. Special Cases

In this section, we will discuss several special cases, where the degrees of freedom in power adaptation are somehow restricted. Specifically, we now restrict the system to have constant transmit power and/or equal spatial power allocation.

1) Variable power and equal spatial allocation (VP-EQ): Here the spatial power parameters are fixed to $\{P_j = 1/N_{\rm t}\}_{j=1}^{N_{\rm t}}$. Thus the BER in (16) is expressed as

$$\text{BER}_{\text{eq}} = 0.2\left(\frac{N_{\rm t}}{N_{\rm t}+\gamma(\tilde{\boldsymbol{\beta}})\sigma^2}\right)^{N_{\rm t}N_{\rm r}} \exp\left(-\frac{\gamma(\tilde{\boldsymbol{\beta}})\sum_{j=1}^{N_{\rm t}}\tilde{\beta}_j}{N_{\rm t}+\gamma(\tilde{\boldsymbol{\beta}})\sigma^2}\right). \tag{34}$$

We can obtain the optimal $\gamma^\star_{\text{eq}}$ by solving the following problem for given $\tilde{\boldsymbol{\beta}}$:

$$\begin{aligned} &\underset{\gamma\geq 0}{\text{minimize}} \quad \gamma \\ &\text{subject to} \quad \text{BER}_{\text{eq}} \leq \text{BER}_{\text{tgt}} \end{aligned}$$

Since (34) is a monotonically decreasing function of γ, the optimal γ gives

$$\text{BER}_{\text{eq}} = \text{BER}_{\text{tgt}}. \tag{35}$$

To solve for γ from (35), we define η as

$$\eta \triangleq \frac{N_{\rm t}}{N_{\rm t}+\gamma\sigma^2}. \tag{36}$$

Hence, substituting (34) and (36) into (35), we obtain

$$(\eta^\star)^{N_{\rm t}N_{\rm r}} e^{b\eta^\star} = 5\text{BER}_{\text{tgt}} e^b$$

where according to (11),

$$b \triangleq \frac{\sum_{j=1}^{N_{\rm t}}\tilde{\beta}_j}{\sigma^2} = \frac{\|\hat{\mathbf{H}}\|_F^2}{(1+\sigma_e^2)\sigma_e^2}. \tag{37}$$

The solution of $\eta^\star$ is thus given by the Lambert W function [24] as

$$\eta^\star = \frac{N_{\rm t}N_{\rm r}}{b} W\left(\frac{b}{N_{\rm t}N_{\rm r}}(5\text{BER}_{\text{tgt}} e^b)^{\frac{1}{N_{\rm t}N_{\rm r}}}\right) \tag{38}$$

where $W(\cdot)$ denotes the principal branch of the Lambert W function, whose value can be accurately calculated [24]. Since $W(x)$ is a monotonic function of x for $x \geq 0$, the value of $\eta^\star$ is unique. Generally, $\text{BER}_{\text{tgt}} < 0.2$, then $\eta^\star$ is shown to be less than 1 as follows:

$$\eta^\star < \frac{N_{\rm t}N_{\rm r}}{b} W\left(\frac{b}{N_{\rm t}N_{\rm r}} e^{\frac{b}{N_{\rm t}N_{\rm r}}}\right) = 1.$$

With the value of $\eta^\star$ less than 1, we can obtain positive $\gamma^\star_{\text{eq}}$ from (36) as

$$\gamma^\star_{\text{eq}} = \frac{N_{\rm t}}{\sigma^2}\left(\frac{1}{\eta^\star} - 1\right). \tag{39}$$

Thus, for the VP-EQ case, (38) and (39) provide the closed-form formulae to calculate optimal $\gamma^\star_{\text{eq}}$. After we obtain $\gamma^\star_{\text{eq}}$, we can follow the same procedures described in Section III-B to calculate the optimal thresholds for our variable-power variable-rate policy.

2) Constant power and spatial power allocation (CP-NE): Under this scheme, we determine the constellation size and spatial power parameters by using the BER minimization results in Appendix A. The procedure can be summarized as follows.

(i) Initially set $M = M_1$ (the largest constellation).
(ii) Use (14) to compute γ with the fixed transmit power and the constellation size M.
(iii) Solve for λ based on (25) by letting $\gamma^\star = \gamma$, and then substitute the obtained λ into (26) to calculate the optimal spatial power parameters.
(iv) Calculate the BER using (16). If BER $\leq \text{BER}_{\text{tgt}}$, the optimal constellation size is set equal to M, otherwise reduce M to a smaller size and repeat from step (ii).

3) Constant power and equal spatial allocation (CP-EQ): The only parameter to be adjusted is the modulation level. The optimal modulation is

$$M = \arg\max_{M\in\{M_l\}_{l=1}^{L+1}} \text{BER}_{\text{eq}} \leq \text{BER}_{\text{tgt}}. \tag{40}$$

where BER_{eq} is given in (34). Equation (40) is solved by evaluating BER_{eq} starting from the largest constellation size.

IV. Numerical Results

In this section, we present numerical results to show the superiority of the proposed variable-rate variable-power with spatial power allocation (VP-NE) adaptation policy. For comparison, we also provide the results of the 3 restricted-methods described in Section III-C and the existing methods from [10] (Yu et al.), [7] (Ko et al.), and [15] (Zhou et al.). The practical issue of the peak power constraint is also addressed.

We assume the set of MQAM constellation is $\{0, 4, 16, 64, 256\}$ and $\text{BER}_{\text{tgt}} = 10^{-3}$. This target BER value has been considered as the QoS requirement for voice communications. We have also obtained similar numerical results for smaller target BERs, but omitted to present here for brevity. In the following figures, SNR is defined as $\bar{S}/\sigma_n^2$ and a system with $N_{\rm t}$ transmit antennas and $N_{\rm r}$ receive antennas is denoted by $N_{\rm t}\times N_{\rm r}$ system. The ASE and average BER are evaluated respectively by [2]

$$\text{ASE} = E_{\hat{\mathbf{H}}}[r\log_2(M(\tilde{\boldsymbol{\beta}}))] \tag{41}$$

$$\overline{\text{BER}} = \frac{E_{\mathbf{H},\hat{\mathbf{H}}}[r\log_2(M(\tilde{\boldsymbol{\beta}}))\text{BER}_{\text{MQAM}}(M(\tilde{\boldsymbol{\beta}}), S(\tilde{\boldsymbol{\beta}}), P_j(\tilde{\boldsymbol{\beta}}), \boldsymbol{\beta})]}{E_{\hat{\mathbf{H}}}[r\log_2(M(\tilde{\boldsymbol{\beta}}))]} \tag{42}$$

where the expectation is averaged over 500 000 channel realizations generated by the channel model described in Section II-A, and $\text{BER}_{\text{MQAM}}(\cdot,\cdot,\cdot,\cdot)$ is a BER expression for MQAM.

A. Performance Comparison

Fig.2 and Fig.3 compare the ASE and average BER of variable-rate system versus SNR with different power adaptation policies respectively. A 2×1 system with Alamouti code ($r = 1$) [12] is considered. The CSIT quality is assumed to be perfect. As shown in the Fig.2, the proposed VP-NE strategy significantly improves the ASE. As expected, restricting the degree of freedom of power adaptation either in space or time results in considerable ASE degradation. Among the existing methods, Yu et al. and Zhou et al. are equivalent to the VP-EQ and CP-NE strategies respectively for the system setups considered in Figs.2 and 3, hence yielding the same ASE as those two strategies. Ko et al. method is basically a constant-power in time and equal-power in space approach, but with additional threshold optimization. Thus it achieves better ASE performance than the CP-EQ strategy described in Section III-C. In Fig.3, we evaluate the average BER by substituting the BER upper bound in (13) into (42). As seen, the target BER is fulfilled by the variable-power schemes and Ko et al..

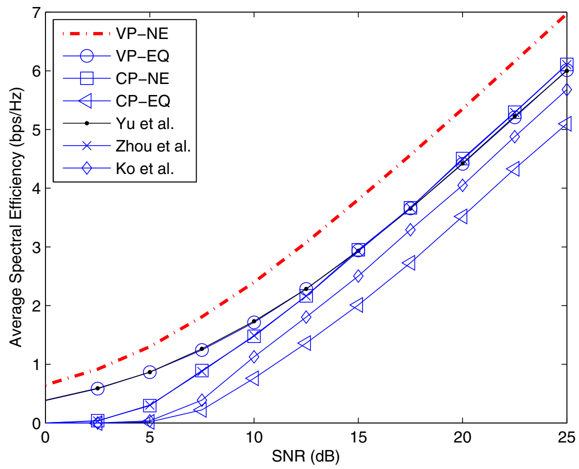

Fig. 2. Average spectral efficiency of 2×1 variable-rate system for different power adaptation strategies with Alamouti code ($r = 1$) and $\sigma_e^2 = 0$.

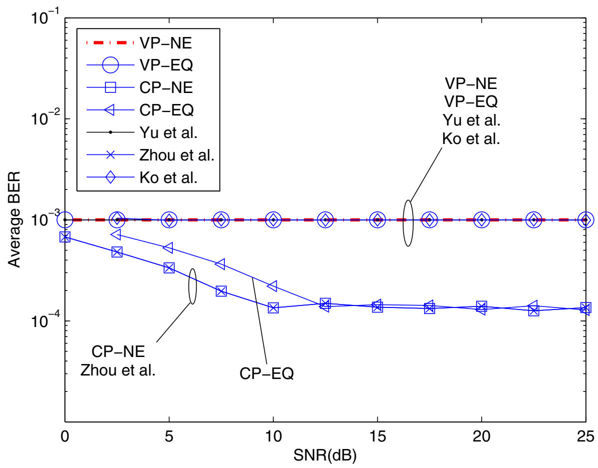

Fig. 3. BER performance of 2×1 variable-rate system for different power adaptation strategies with Alamouti code ($r = 1$) and $\sigma_e^2 = 0$.

However, the constant-power schemes (including CP-NE, CP-EQ and Zhou et al.) have BER lower than the target BER due to the rate discretization and constant power restriction. Notice that even the lowest constellation size cannot be supported at 0dB for the CP-EQ method. So no BER performance is given at that point.

Fig.4 plots the ASE of a 4×1 system for the different adaptation policies with imperfect CSIT, where $\sigma_e^2 = 0.2$. The H_4 code with $r = 3/4$ [16] is adopted. In the figure, we also include the ASE performance of MIMO systems that use the two largest eigen-beams with the full-rate Alamouti code for transmission, denoted as 2D-VP-NE. This 2D system was suggested by Zhou et al. in [15]. In Fig.4, we observe the similar superiority of the VP-NE (2D-VP-NE) over Ko et al. (Zhou et al.) as found in Fig.2. We did not include the method from Yu et al. in Fig.4, because the imperfection assumption on the channel model therein is different from here. The average BER performance is also similar to what was reported in Fig.3, thus omitted. Regarding the online computational complexity of the proposed VP-NE scheme, the extra cost is

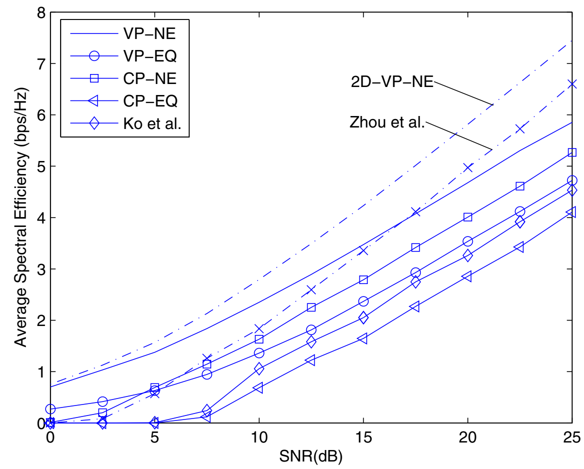

Fig. 4. Average spectral efficiency for 4×1 variable-rate system for different power adaptation strategies with $\sigma_e^2 = 0.2$. For the solid curves, H_4 code ($r = 3/4$) is used. For the dash curves, the two largest eigen-beams with Alamouti code ($r = 1$) is used for transmission.

the calculation of $\gamma^\star$ for the given CSIT, as compared to Zhou et al. Nevertheless, this calculation can be done efficiently via one-dimensional root-finding of a monotonic function by bisection or Newton's method, as described in Algorithm 2 in Section III-A. The complexity of this root-finding is small in comparison with the eigen-decomposition of $\hat{\mathbf{H}}^H\hat{\mathbf{H}}$.

Fig.5 and Fig.6 respectively plot the ASE and BER of the 2×1 system using the VP-NE versus SNR for $\sigma_e^2 = 0, 0.05, 0.1, 0.2, 0.5, 1$. As shown in Fig.5, the ASE increases with SNR, but decreases as σ_e^2 increases. Fig.6 plots the average BER upper bound and accurate BER, which are obtained by substituting the upper bound in (13) and the accurate BER formula in [3, Eq.(46)] into (42) respectively. It is shown that the average BER obtained from the upper bound equals the target BER for different σ_e^2. However, we can observe gaps between the target BER and the actual BER obtained from the accurate BER formula. This is because the design is based on the upper bound approximation. One can also notice that the gaps increase as the SNR increases, and decrease as the σ_e^2 increases. The reason is that the BER approximation in (13) is more accurate when low-order constellation is used, as reported in Fig.1 of [15]. When the SNR is low or σ_e^2 is large, the probability of choosing the low-order modulation increases (resulting in lower ASE in Fig.5). Hence, the BER approximation is getting closer to the actual BER and resulting in narrower gap.

B. Peak-to-Average-Power Ratio (PAPR) Issue

The proposed VP-NE scheme dynamically adapts the total transmit power in accordant with the instantaneous CSI. The transmit power allocation may be too large to cause nonlinear distortion in power amplification that degrades transmission reliability. We will illustrate in this subsection that the proposed power adaptation has moderate peak-to-average-power ratio (PAPR). Also, we will incorporate the power allocation algorithm with a peak power constraint so that the proposed variable-power strategy has a mechanism to control the tempo-

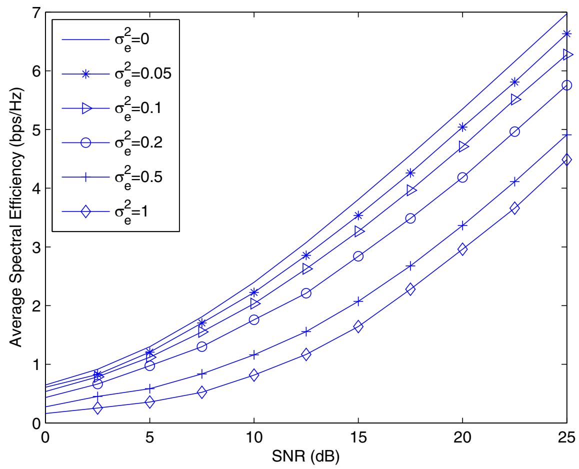

Fig. 5. Average spectral efficiency of 2×1 variable-rate system with the proposed VP-NE strategy and Alamouti code for different estimation error variances.

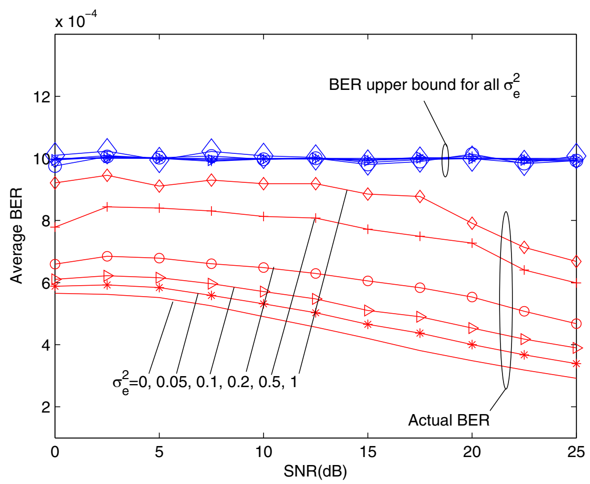

Fig. 6. BER performance of 2×1 variable-rate system with the proposed VP-NE strategy and Alamouti code for different estimation error variances.

ral power subject to a given PAPR. First, the temporal power versus $\gamma^\star$ for the VP-NE policy at SNR=20dB and SNR=5dB are given in Fig.7 and Fig.8, respectively. The system configuration is the same as that of Fig.5 with $\sigma_e^2 = 0.1$. The temporal power of 1,000 random channel realizations is plotted in the figures. An inset with the range of $\gamma^\star$ in the low value region is also plotted in each figure for better illustration. As observed in Fig.7, the range of $\gamma^\star$ is partitioned into 5 regions, with the thresholds $\{\gamma_l\}_{l=1}^4 = \{1.18, 4.72, 18.87, 75.49\}$. The temporal power is a piece-wise linear function of $\gamma^\star$ in accordance with (32c). The constellations corresponding to the partitions are sorted in descending order. All $\gamma^\star$ values have been used for data transmission, except for those larger than 75.49, resulting in high ASE. In contrast, at SNR=5dB, although the values of $\gamma^\star$ are all the same as that of SNR=20dB (since the inner problem (24) is independent of SNR), the optimal thresholds are $\{\gamma_l\}_{l=1}^4 = \{0.08, 0.31, 1.25, 4.99\}$, which are much smaller than that of SNR=20dB in order to satisfy the average power constraint (32b) for larger noise variance σ_n^2.

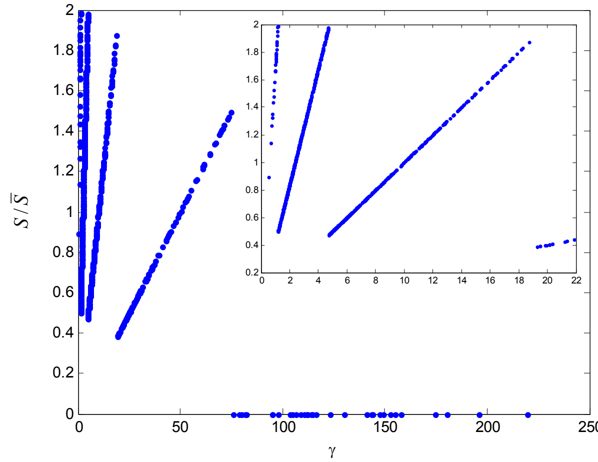

Fig. 7. Normalized temporal power versus $\gamma^\star$ value of 2×1 variable-rate system with the proposed VP-NE strategy and Alamouti code for SNR=20dB and $\sigma_e^2 = 0.1$.

As shown in Fig.8, a large number of realizations falls in the region of "no transmission". Note that none of the 1,000 channel realizations falls in the two regions of highest rate, but mostly fall in the two regions of lowest rate. These results explain why higher ASE can be achieved by the VP-NE at higher SNR's in Fig.5.

Fig.7 and Fig.8 demonstrate that the VP-NE has moderate PAPR that is less than 3dB and 6dB at high and low SNR's respectively. In order to further control the PAPR, we can amend the VP-NE scheme to take into account the additional peak power constraint $S(\tilde{\boldsymbol{\beta}}) \leq S_{\max}$ as follows. Based on (32c) and the observations from Figs.7 and 8, we know that the temporal power must hit the peak only at the boundaries of $\{\gamma_l\}$, and nowhere else. Then we can revise the boundaries as $\gamma_l^{\text{new}} = \min\{\gamma_l, \frac{1.5 S_{\max}}{(M_l-1) r \sigma_n^2}\}$, for $l = 1, \ldots, L$. By doing so, we still maintain the BER target because we did not change the value of $\gamma^\star$. However, the ASE will be reduced and so is the average power from (32a) and (32b).

Fig.9 plots the temporal power versus $\gamma^\star$ at SNR=5dB with the additional peak power constraint of $S(\tilde{\boldsymbol{\beta}}) \leq 3\bar{S}$. The system parameters are the same as those in Fig.8, but the boundaries have been modified to $\{\gamma_l^{\text{new}}\}_{l=1}^4 = \{0.06, 0.23, 0.95, 4.74\}$ to satisfy the peak power constraint. In the sub-figure, we compare the ASE with and without the peak power constraint when the SNR varies from 0dB to 25dB. As seen, the peak power constraint reduces the ASE in the low SNR region.

V. Conclusion

In this paper, we have proposed the joint rate and spatio-temporal power adaptation scheme for OSTBC/OSTBC-BF MIMO systems with imperfect CSIT. The proposed transmitter optimally adjusts the signal constellation, temporal power, and spatial power allocation to maximize the average spectral efficiency, subject to a target bit-error-rate and an average power constraint. By introducing a new variable, the so-called ESNMR, we have obtained the rate-selection policy by partitioning the range of the ESNMR with optimal thresholds. A closed-form temporal power control policy and a simple

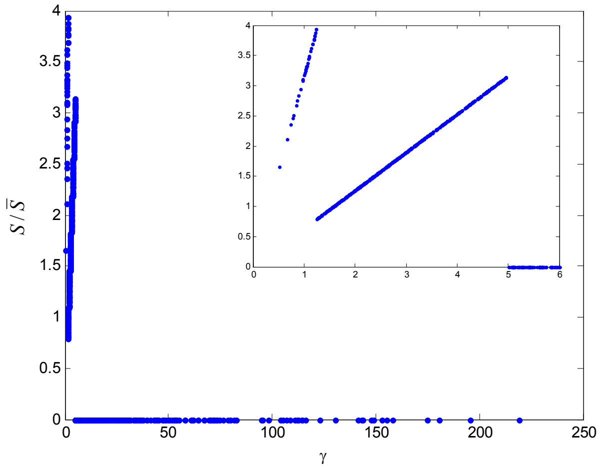

Fig. 8. Normalized temporal power versus $\gamma^\star$ value of 2×1 variable-rate system with the proposed VP-NE strategy and Alamouti code for SNR=5dB and $\sigma_e^2 = 0.1$.

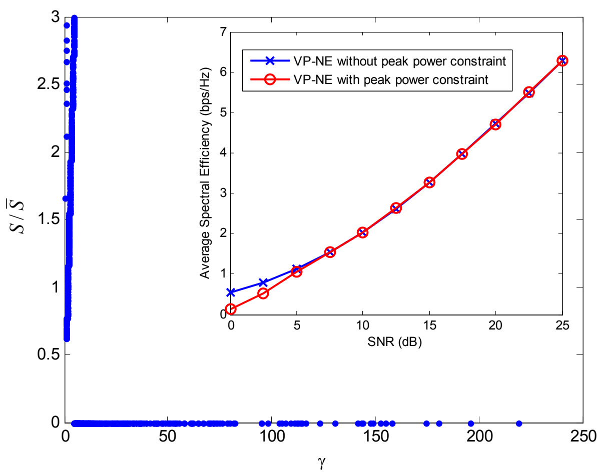

Fig. 9. Normalized temporal power versus $\gamma^\star$ value of 2×1 variable-rate system with the proposed VP-NE strategy and Alamouti code, and with peak power constraint: $S(\tilde{\boldsymbol{\beta}}) \leq 3\bar{S}$, for SNR=5dB and $\sigma_e^2 = 0.1$. In the sub-figure, average spectral efficiency of the VP-NE is plotted versus SNR with/without the peak power constraint.

spatial power allocation algorithm have also been obtained. Compared to adaptive systems with restricted freedoms on power adaptation, our adaptation scheme significantly improves the ASE. The additional peak power constraint can be incorporated into the proposed scheme. The simulation results show that the ASE of the VP-NE scheme with an additional peak power constraint may be reduced in the low SNR region.

Appendix A
Solution for the Inner Optimization Problem

In this Appendix, we derive the solution to the inner optimization problem of (24). First, the BER constraint is modified by taking the natural log of both sides of the constraint, we have

$$\widetilde{\text{BER}} \leq \epsilon = \log(\text{BER}_{\text{tgt}}) - \log 0.2 \tag{43}$$

where

$$\widetilde{\text{BER}} = -\sum_{j=1}^{N_\text{t}} \left[N_\text{r} \log(1 + \gamma\sigma^2 P_j) + \frac{\gamma\tilde{\beta}_j P_j}{1 + \gamma\sigma^2 P_j} \right] \tag{44}$$

Note that (44) is a convex function of $\{P_j\}$ for given γ and a decreasing function of γ for given $\{P_j\}$. These properties suggest that the constrained problem of (24) can be interpreted or solved as a maximin problem as follows. We first minimize $\widetilde{\text{BER}}$ with respect to $\{P_j\}$ for given γ subject to the spatial power constraints. If there exist nonzero γ and $\{P_j\}$ yielding $\widetilde{\text{BER}}$ less than ϵ, then we can reduce the value of γ to increase $\widetilde{\text{BER}}$. The minimum value of γ that makes $\widetilde{\text{BER}}$ reach ϵ is the optimal value of (24). Mathematically, the problem can be rewritten as

$$\underset{\gamma \geq 0}{\text{maximize}} \ \underset{\{P_j\}}{\text{minimize}} \ \widetilde{\text{BER}}$$

$$\text{subject to} \qquad \widetilde{\text{BER}} \leq \epsilon, \sum_{j=1}^{N_\text{t}} P_j = 1, P_j \geq 0. \tag{45}$$

The solution to the inner convex minimization problem of (45) can be obtained by the KKT conditions [21]: $\sum P_j = 1, P_j \geq 0, -\frac{N_\text{r}\gamma\sigma^2}{1+\gamma\sigma^2 P_j} - \frac{\gamma\tilde{\beta}_j}{(1+\gamma\sigma^2 P_j)^2} + \eta - \mu_j = 0, \mu_j \geq 0, \mu_j P_j = 0$, where $j = 1, \ldots, N_\text{t}$, η and $\{\mu_j\}$ are the Lagrangian multipliers for the sum power constraint and the inequality constraints respectively. From the complementary slackness condition, we know that if $P_j > 0$, then $\mu_j = 0$. Then applying the gradient vanishing condition, we have

$$\frac{N_\text{r}\gamma\sigma^2}{1 + \gamma\sigma^2 P_j} + \frac{\gamma\tilde{\beta}_j}{(1 + \gamma\sigma^2 P_j)^2} = \eta.$$

Let us define a parameter λ as

$$\lambda = \frac{\eta}{\gamma} = \frac{N_\text{r}\sigma^2}{1 + \gamma\sigma^2 P_j} + \frac{\tilde{\beta}_j}{(1 + \gamma\sigma^2 P_j)^2}. \tag{46}$$

Solving (46) for P_j subject to the nonnegative condition give

$$P_j = \max\left\{0, \frac{1}{\gamma\sigma^2}\left(\mathcal{I}_j(\lambda) - 1\right)\right\} \tag{47}$$

where

$$\mathcal{I}_j(\lambda) = \frac{\sqrt{N_\text{r}^2\sigma^4 + 4\tilde{\beta}_j\lambda} + N_\text{r}\sigma^2}{2\lambda}. \tag{48}$$

Assume the number of eigen-beams with nonzero power is $\bar{N}_\text{t}$ (whose value is determined by Theorem 1). From (47) and the sum power constraint $\sum_{j=1}^{\bar{N}_\text{t}} P_j = 1$, we obtain

$$\gamma = \frac{1}{\sigma^2}\left(\sum_{j=1}^{\bar{N}_\text{t}} \mathcal{I}_j(\lambda) - \bar{N}_\text{t}\right) \tag{49}$$

The λ parameter of (47) and (49) can be determined as follows. The optimal $\{P_j\}$ and γ values of the maximin problem (45) will set $\widetilde{\text{BER}}$ equal to the maximum allowable value ϵ. That is

$$\widetilde{\text{BER}} = \epsilon. \tag{50}$$

Substituting (44) and (47) into (50) obtains

$$F_{\bar{N}_\text{t}}(\lambda) = \log\frac{0.2}{\text{BER}_{\text{tgt}}} - \sum_{j=1}^{\bar{N}_\text{t}} \left(N_\text{r} \log \mathcal{I}_j(\lambda) + \frac{\mathcal{I}_j(\lambda)\tilde{\beta}_j - \tilde{\beta}_j}{\mathcal{I}_j(\lambda)\sigma^2} \right). \tag{51}$$

The value of λ is obtained by solving the root of $F_{\bar{N}_\text{t}}(\lambda)$ in (51).

The above BER minimization can be applied to the case of constant transmit power and given constellation size with spatial power allocation. Under this scheme, according to (14), the γ is fixed. The λ value for computing the optimal spatial power parameters in (47) can be obtained by solving (49).

Appendix B
Numerical Calculation of γ_0 in (31)

From [25], the joint pdf of the ordered eigenvalues $\{\zeta_i\}$ of the Wishart matrix $\mathbf{H}^H\mathbf{H}$, where the entries of $\mathbf{H}$ are i.i.d. complex Gaussian with zero mean and unit variance, is given as

$$f_{\boldsymbol{\zeta}}(\zeta_1,\ldots,\zeta_{m_0}) = \frac{1}{K_{m_0,n_0}} e^{-\sum_i \zeta_i} \prod_i \zeta_i^{n_0-m_0} \prod_{i<j}(\zeta_i-\zeta_j)^2 \tag{52}$$

where $m_0 = \min\{N_\mathrm{t}, N_\mathrm{r}\}$, $n_0 = \max\{N_\mathrm{t}, N_\mathrm{r}\}$, $K_{m_0,n_0} = \prod_{i=1}^{m_0}(m_0-i)!(n_0-i)!$ is a normalized factor. According to our channel estimation model and (11), the nonzero eigenvalues $\{\hat{\zeta}_i\}$ of $\hat{\mathbf{H}}^H\hat{\mathbf{H}}$ can be expressed in terms of $\{\zeta_i\}$ as $\hat{\zeta}_i = \zeta_i(1+\sigma_e^2)$. Then the nonzero entries of $\tilde{\boldsymbol{\beta}}$ can be expressed in terms of $\{\zeta_i\}$ as

$$\tilde{\beta}_i = \frac{\hat{\zeta}_i}{(1+\sigma_e^2)^2} = \frac{\zeta_i}{1+\sigma_e^2}, \quad i=1,\ldots,m_0. \tag{53}$$

Hence, the pdf $f_{\tilde{\boldsymbol{\beta}}}(\tilde{\boldsymbol{\beta}})$ is obtained as

$$f_{\tilde{\boldsymbol{\beta}}}(\tilde{\beta}_1,\ldots,\tilde{\beta}_{m_0}) = (1+\sigma_e^2)^{m_0} f_{\boldsymbol{\zeta}}(\zeta_1,\ldots,\zeta_{m_0})|_{\zeta_i=\tilde{\beta}_i(1+\sigma_e^2)}. \tag{54}$$

According to Gauss-Laguerre quadrature formula [23], the integration in (31) can be evaluated as

$$\sum_{i_1=1}^{N_p}\cdots\sum_{i_{m_0}=1}^{N_p} w_{i_1}\ldots w_{i_{m_0}}\phi(\mathbf{z_i})\frac{r\sigma_n^2}{1.5}(\gamma_0-\gamma^\star(\mathbf{z_i}))^+ \tag{55}$$

where $\{w_i\}$ denote the weights associated with zeros $\{z_i\}$ of the one-dimensional N_pth order Laguerre polynomial, $\mathbf{z_i} = (z_{i_1},\cdots,z_{i_{m_0}})$ denotes the vector of zeros associated with the index vector $\mathbf{i} = (i_1,\cdots,i_{m_0})$, and $\phi(\mathbf{z_i})$ is given as

$$\phi(\mathbf{z_i}) = \frac{1}{m_0!K_{m_0,n_0}}\prod_{l=1}^{m_0}\left[\left(\sum_{j=l}^{m_0}\frac{z_{i_j}}{j}\right)^{n_0-m_0}\prod_{j=l}^{m_0-1}\left(\sum_{k=l}^{j}\frac{z_{i_k}}{k}\right)^2\right] \tag{56}$$

and $\gamma^\star(\mathbf{z_i})$ in (55) is obtained by assigning $\{\tilde{\beta}_j\}$ with the following values

$$\tilde{\beta}_j = \begin{cases}\frac{\sum_{k=j}^{m_0}(z_{i_k}/k)}{(1+\sigma_e^2)} & \text{for} \quad j=1,\ldots,m_0\\ 0 & \text{for} \quad j=m_0+1,\ldots,N_\mathrm{t}\end{cases} \tag{57}$$

and following the algorithm 2 proposed in Section III-A. We use bisection method to find the value of γ_0 by comparing the computed expectation value based on (55) with the power budget $\bar{S}$.

Appendix C
Numerical Calculation of μ in (33)

The average power constraint (32b) can be rewritten as

$$\psi(\mu) = \int \frac{(M_{I(\gamma^\star)}-1)r\sigma_n^2\gamma^\star}{1.5} f_{\tilde{\boldsymbol{\beta}}}(\tilde{\boldsymbol{\beta}})d\tilde{\boldsymbol{\beta}} = \bar{S} \tag{58}$$

where $I(\gamma^\star)$ is an indicator function to indicate which region of γ that $\gamma^\star$ belongs to, defined as

$$I(\gamma^\star) = l, \quad \mu t_{l-1} \le \gamma^\star < \mu t_l.$$

According to (55), we can calculate the integration in (58) as

$$\sum_{i_1=1}^{N_p}\cdots\sum_{i_{m_0}=1}^{N_p} w_{i_1}\ldots w_{i_{m_0}}\phi(\mathbf{z_i})\frac{(M_{I(\gamma^\star(\mathbf{z_i}))}-1)r\sigma_n^2\gamma^\star(\mathbf{z_i})}{1.5}.$$

To check the condition of existence of μ, we first evaluate $\psi(\infty)$ as

$$\psi(\infty) = \sum_{i_1=1}^{N_p}\cdots\sum_{i_{m_0}=1}^{N_p} w_{i_1}\ldots w_{i_{m_0}}\phi(\mathbf{z_i})\frac{(M_1-1)r\sigma_n^2\gamma^\star(\mathbf{z_i})}{1.5}.$$

If $\psi(\infty) > \bar{S}$, μ exists. Then we use the bisection method to refine the value of μ to satisfy the average power constraint.

References

[1] A. J. Goldsmith and S.-G. Chua, "Variable-rate variable-power MQAM for fading channels," *IEEE Trans. Commun.*, vol. 45, no. 10, pp. 1218–1230, Oct. 1997.

[2] S. T. Chung and A. J. Goldsmith, "Degrees of freedom in adaptive modulation: a unified view," *IEEE Trans. Commun.*, vol. 49, no. 9, pp. 1561–1571, Sep. 2001.

[3] B. Choi and L. Hanzo, "Optimum mode-switching-assisted constant-power single- and multicarrier adaptive modulation," *IEEE Trans. Veh. Technol.*, vol. 52, no. 3, pp. 536–560, May 2003.

[4] H. Zhu and J. Wang, "Chunk-based resource allocation in OFDMA systems–part I: chunk allocation," *IEEE Trans. Commun.*, vol. 57, no. 9, pp. 2734–2744, Sep. 2009.

[5] L. T. Ong, M. Shikh-Bahaei, and J. A. Chambers, "Variable-rate and variable power MQAM system based on Bayesian bit error rate and channel estimation techniques," *IEEE Trans. Commun.*, vol. 56, no. 2, pp. 177–182, Feb. 2008.

[6] S. Zhou and G. B. Giannakis, "Optimal transmitter eigen-beamforming and space-time block coding based on channel mean feedback," *IEEE Trans. Signal Process.*, vol. 50, no. 10, pp. 2599–2613, Oct. 2002.

[7] Y. Ko and C. Tepedelenlioglu, "Orthogonal space-time block coded rate-adaptive modulation with outdated feedback," *IEEE Trans. Wireless Commun.*, vol. 5, no. 2, pp. 290–295, Feb. 2006.

[8] D. V. Duong and G. E. Oien, "Optimal pilot spacing and power in rate-adaptive MIMO diversity systems with imperfect CSI," *IEEE Trans. Wireless Commun.*, vol. 6, no. 3, pp. 845–851, Mar. 2007.

[9] J. Huang and S. Signell, "On performance of adaptive modulation in MIMO systems using orthogonal space-time block codes," *IEEE Trans. Veh. Technol.*, vol. 58, no. 8, pp. 4238–4247, Oct. 2009.

[10] X. Yu, S.-H. Leung, W. H. Mow, and W.-K. Wong, "Performance of variable-power adaptive modulation with space-time coding and imperfect CSI in MIMO systems," *IEEE Trans. Veh. Technol.*, vol. 58, no. 4, pp. 2115–2120, May 2009.

[11] J. Huang and S. Signell, "On spectral efficiency of low-complexity adaptive MIMO systems in Rayleigh fading channel," *IEEE Trans. Wireless Commun.*, vol. 8, no. 9, pp. 4369–4374, Sep. 2009.

[12] E. G. Larrsson and P. Stoica, *Space-Time Block Coding for Wireless Communications*. Cambridge University Press, 2003.

[13] G. Jongren, M. Skoglund, and B. Ottersten, "Combining beamforming and orthogonal space-time block coding," *IEEE Trans. Inf. Theory*, vol. 48, no. 3, pp. 611–627, Mar. 2002.

[14] J. W. Huang, E. K. S. Au, and V. K. N. Lau, "Precoder design for space-time coded MIMO systems with imperfect channel state information," *IEEE Trans. Wireless Commun.*, vol. 7, no. 6, pp. 1977–1981, June 2008.

[15] S. Zhou and G. B. Giannakis, "Adaptive modulation for multiantenna transmissions with channel mean feedback," *IEEE Trans. Wireless Commun.*, vol. 3, no. 5, pp. 1626–1636, Sep. 2004.

[16] V. Tarokh, H. Jafarkhani, and A. R. Calderbank, "Space-time block coding for wireless communications: performance results," *IEEE J. Sel. Areas Commun.*, vol. 17, no. 3, pp. 451–460, Mar. 1999.

[17] E. G. Larsson, "Diversity and channel estimation errors," *IEEE Trans. Commun.*, vol. 52, no. 2, pp. 205–208, Feb. 2004.

[18] S. Kay, *Fundamentals of statistical signal processing: estimation theroy*. Prentice-Hall, 1993.

[19] H. Shin and J. H. Lee, "Performance analysis of space-time block codes over keyhole Nakagami-m fading channels," *IEEE Trans. Veh. Technol.*, vol. 53, no. 2, pp. 351–362, Mar. 2004.

[20] J. G. Proakis, *Digital Communications*. McGraw-Hill, 2001.

[21] S. Boyd and L. Vandenberghe, *Convex Optimization*. Cambridge University Press, 2004.

[22] E. R. Pinch, *Optimal Control and the Calculus of Variations*. Oxford University Press, 1993.

[23] P. J. Davis and P. Rabinowitz, *Methods of Numerical Integration*. Academic Press, 1975.

[24] R. Corless, G. Gonnet, D. Hare, D. Jeffrey, and D. Knuth, "On the lambertw function," *Advances in Computational Mathematics*, vol. 5, pp. 329–359, Dec. 1996.

[25] I. E. Telatar, "Capacity of multi-antenna Gaussian channels," *European Trans. Commun.*, vol. 10, no. 6, pp. 585–595, Nov.-Dec. 1999.

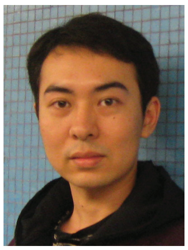

Quan Kuang received the Ph.D. degree in electrical engineering from the City University of Hong Kong, China, in 2011. Since February 2011, he has been with the Institute of Telecommunications in the University of Stuttgart, Germany, as a research staff member. From 2004 to 2007, he was a lecturer at the Guilin University of Electronic Technology, China. His interests include space-time coding, beamforming, adaptive transmission, and resource allocation in multi-cell cellular networks.

Shu-Hung Leung received his first class honors B.Sc. degree in electronics from the Chinese University of Hong Kong in 1978, and his M.Sc. and Ph.D. degrees, both in electrical engineering, from the University of California at Irvine in 1979 and 1982, respectively. From 1982 to 1987, he was an Assistant Professor with the University of Colorado at Boulder. Since 1987, he has been with the Department of Electronic Engineering in City University of Hong Kong, where he is currently an Associate Professor. His current research interest is in digital communications, speech signal processing, image processing, and adaptive signal processing. He has received more than twenty research grants from CERG, Croucher Foundation and City University strategic grants and published over 200 technical papers in journals and international conference proceedings. He is now an associate editor of IEEE TRANSACTIONS ON VEHICULAR TECHNOLOGY. He served as Chairmen of the signal processing chapter of the IEEE Hong Kong Section in 2003-04 and as organizing committee member for a number of international conferences. He is listed in the *Marquis Who's Who in Science and Engineering* and *Marquis Who's Who in the World*.

Xiangbin Yu received his Ph.D. in Communication and Information Systems in 2004 from National Mobile Communications Research Laboratory at Southeast University, China. He has been an Associate Professor with the Nanjing University of Aeronautics and Astronautics since May 2006. From April 2010 to April 2011, he worked as a Research Fellow in the Department of Electronic Engineering, City University of Hong Kong, Hong Kong. Dr. Yu served as a technical program committee member of the 2006 Global Telecommunications Conference, the International Conference on Communication Systems in 2008 and 2010, and the 2010 and 2011 Wireless Communications and Signal Processing. He is also a Reviewer for several journals. His research interests include Multi-carrier CDMA, space-time coding, adaptive modulation and space-time signal processing.